Decentralized Secondary Frequency Restoration and Power Sharing Control in Islaned Microgrid Systems

Zhijie Lian[1,2], Fanghong Guo[3], Changyun Wen[2]

1. Energy Research Institute @NTU, Interdisciplinary Graduate School, Nanyang Technological University, Singapore
E-mail: zhijie003@e.ntu.edu.sg

2. School of Electrical and Electronic Engineering, Nanyang Technological University, Singapore
E-mail: ecywen@ntu.edu.sg

3. Department of Automation, Zhejiang University of Technology, Hangzhou 310032, China,
E-mail: fhguo@zjut.edu.cn (*corresponding author*)

Abstract: In this paper, a totally decentralized control scheme is proposed to address the secondary frequency restoration and real power sharing problem in AC microgrid (MG) systems. Different from existing centralized or distributed control approaches, no communication among controllers is required with our method, which greatly eases the system implementation cost. It is theoretically proved that the designed decentralized leaky integral controllers can restore the frequency to its nominal value with bounded steady-state error, which can be arbitrarily small by choosing proper control parameters. In addition, the proposed controller can also adjust the real power sharing ratio according to different working conditions. An islanded AC MG test system consisting of 4 distributed generators (DGs) is built in MATLAB Simulink environment and the simulation results validate the effectiveness of proposed decentralized control approach.

Key Words: Decentralized leaky integral control, secondary frequency restoration, power sharing control, microgrid system.

1 Introduction

Microgrid (MG) concept was proposed at the beginning of this century with the growing penetration of renewable energy resources [1]. An MG is a small-scale power system that may consist of conventional generators, renewable resources, energy storage systems and load [2]. It could operate in two different modes, i.e., grid-connected mode and islanded mode. In grid-connected mode, an MG can be controlled as a virtual power plant to import/export power to the main grid. While in islanded mode, other than operating autonomously to maintain the system frequency and voltage, it can also be controlled to share real power economically and enhance power quality [3].

Different control structures have been reported on islanded MG control [3]. The most popular approach is a hierarchical control structure that divides the whole control structure into three layers i.e. primary, secondary and tertiary layers [4]. Primary control, which is the embedded local controller for each of the DGs, is decentralized control in nature. While secondary and tertiary control are usually operated in a microgrid central controller (MGCC), which is in fact a centralized controller. All the required DG information has to be collected, processed in MGCC and the control command has to be sent back to each DG respectively. This centralized controller is at the cost of high computation complexity and heavy communication burden as the system scales up [5]. Apart from the high risk of single-point failure, any add up of new DGs or removal of any existing DGs would require a modification of the MGCC and sometimes may result in an overhaul of the entire control structure.

In order to overcome above disadvantages, distributed control structures have been proposed in recent yaers. It does not require a centralized control unit and the controllers are distributed in each of the local controllers. With only peer-to-peer communication, all the distributed controllers are able to achieve the same goal as what can be achieved by the centralized controller [6]. General control functions in the secondary layer such as distributed frequency and voltage restoration, distributed mitigation of voltage unbalance and harmonics have been addressed in [7] and [8] respectively. Other control functions in the tertiary layer such as distributed economic dispatch have also been reported in [9].

In this paper, we put our emphasis on the secondary control of frequency restoration and real power sharing in an islanded AC MG. Conventionally, such function is realized in a centralized or distributed control architectures. It is noted that the information communication is required in both centralized control and distributed control. However, due to several concerns from the aspects of security, robustness and economic, it is desirable to remove such information communication, resulting in a totally decentralized secondary control structure. Compared to centralized and distributed controllers, decentralized controller only utilizes its own local information to make decision at each single node, see [10] for example. In this way, it could

The work was supported by Zhejiang Provincial Natural Science Foundation of China under Grant No. LQ19F030008.

not only improve the reliability and robustness of power system, but also greatly reduce communication cost. In fact, recently some decentralized controllers have already been applied in power system research works such as in [11, 12, 13]. For instance, in [11], a decentralized PID load frequency control has been used in multi-area power systems. An optimal decentralized control method is proposed for microgrid system in [12] by using linear quadratic regulator, which could work well for frequency restoration but it could not guarantee the power sharing accuracy. In [13], an agent-based decentralized control method is presented, where the system frequency could be regulated to the reference value with tolerant fluctuations and power sharing accuracy brought by droop control function is maintained, i.e., inverse proportional to the droop gains. However, in practice, the power sharing ratio determined by the droop gains could not always be the optimal one, instead, it could be adjusted dynamically due to different working conditions.

Taking above discussions into account, this paper proposes a totally decentralized control scheme for secondary frequency restoration control in islanded MG systems, which is developed based on a leaky integral controller. The proposed approach could not only maintain the system frequency to its nominal value with arbitrarily small steady-state error, but also dynamically adjust the power sharing among DGs without any communication. The stability of overall MG system together with the proposed decentralized controllers is analyzed. Several case studies implemented on an islanded MG system validate the effectiveness of proposed method.

2 Problem formulation and objectives

In this section, the MG model with droop control function is first introduced, based on which the secondary control objective is proposed.

2.1 MG Model

Suppose there are N inverter-based DGs in this islanded MG. Each DG is equipped with a droop-controlled primary controller and operates in a decentralized way [3]. Generally there are three control loops in the primary controller, namely, the voltage control loop, current control loop and droop control loop. The first two loops are to guarantee the voltage and current outputs to track their own references respectively. While the droop control loop is designed to share the real and reactive power outputs among all the DGs according to their pre-defined sharing ratios.

As the main focus of this paper lies in the frequency restoration and real power sharing, in the following, similar to most existing research works [11, 12, 13], we ignore the voltage dynamics and treat them as constants. Then the frequency droop of the i^{th} DG is expressed as

$$\omega_i = \omega^d - k_{P_i}({P_i}^m - {P_i}^d) \tag{1}$$

where ω^d is the desired frequency, k_{P_i} is the droop gain, P_i^m and P_i^d are the measured and desired real power outputs respectively.

Usually the measured P_i^m is obtained through a first-order low-pass filter as

$$\tau_{P_i}\dot{P_i}^m = -{P_i}^m + P_i \tag{2}$$

where τ_{P_i} is the filter time constant, P_i is the real power output of the i^{th} DG.

Substituting (2) into (1), we have

$$\tau_{P_i}\dot{\omega}_i + \omega_i - \omega^d + k_{P_i}(P_i - {P_i}^d) = 0 \tag{3}$$

Eqn. (3) denotes the simplified frequency dynamics of i^{th} DG with primary droop control function.

Note that an MG distribution network is considered as a connected and complex-weighted graph $\mathcal{G} = (\mathcal{V}, \xi)$ with nodes $\mathcal{V}$ being the buses and edges ξ being the line impedance. Consider a network with N DGs together with their corresponding local loads, and M transmission lines, and let Y_{ik} be the admittance between the i^{th} and k^{th} DG bus, which is defined as $Y_{ik} = G_{ik} + jB_{ik} \in \mathbb{C}$, where $G_{ik} \in \mathbb{R}$ and $B_{ik} \in \mathbb{R}$ are the conductance and susceptance respectively. If there is no connection between the i^{th} and k^{th} DG bus, we define $Y_{ik} = 0$. We also define $G_{ii} = \sum_{k\in\mathcal{N}_i} G_{ik}$, $B_{ii} = \sum_{k\in\mathcal{N}_i} B_{ik}$. In addition, we define $\mathcal{B} \in \mathbb{R}^{N\times M}$ as the incidence matrix of the MG system with N DGs and M transmission lines.

Based on power balance relations, the real power injected (or absorbed) into (or from) the i^{th} DG bus in the MG network $\hat{P}_i$ is

$$\hat{P}_i = {V_i}^2 G_{ii} - \sum_{k\in\mathcal{N}_i} V_i V_k \left|Y_{ik}\right| \cos(\delta_i - \delta_k - \phi_{ik}) \tag{4}$$

where V_i and δ_i are the voltage magnitude and the phase angle of the i^{th} DG bus, $|Y_{ik}|$ is the magnitude of the admittance Y_{ik}, *i.e.*, $|Y_{ik}| = \sqrt{{G_{ik}}^2 + {B_{ik}}^2}$, ϕ_{ik} is the admittance angle of Y_{ik}, *i.e.*, $\phi_{ik} = \phi_{ki} = \arctan(B_{ik}/G_{ik})$. If the power transmission lines of the MG network are lossless, i.e., $G_{ik} = 0$, $Y_{ik} = jB_{ik}$, $\phi_{ik} = \phi_{ki} = -\frac{\pi}{2}$, $\forall i \in N, k \in \mathcal{N}_i$, then (4) becomes

$$\hat{P}_i = \sum_{k\in\mathcal{N}_i} V_i V_k \left|B_{ik}\right| \sin(\delta_i - \delta_k) \tag{5}$$

As the voltage dynamics is not considered in this paper, hence (5) can be also rewritten as

$$\hat{P}_i = \sum_{k\in\mathcal{N}_i} H_{ik} \sin(\delta_i - \delta_k) \tag{6}$$

where $H_{ik} = V^2 \left|B_{ik}\right|$ with $V_i = V_k = V$ being a constant voltage amplitude in (5).

In addition, denote the local load in bus i as P_{L_i}, then the power output from the i^{th} DG can be obtained as

$$P_i = P_{L_i} + \hat{P}_i \tag{7}$$

2.2 Objectives

It is well known that the frequency of the whole MG system under primary controller with the frequency droop function

(1) will be synchronized to a steady-state value ω_{ss}, i.e.,

$$\omega_{ss} = \omega^d + \frac{\sum_{i=1}^{N} k_{P_i}(P_i^d - P_i)}{N}. \quad (8)$$

Clearly Eqn. (8) indicates that as long as $\sum_{i=1}^{N} k_{P_i}(P_i^d - P_i) \neq 0$, the synchronized frequency will deviate from its nominal value ω^d. Hence the first objective of this paper is to design a secondary control to restore the frequency, i.e.,

$$\lim_{t\to\infty}\omega_i(t) = \omega^d, \forall i = 1, \cdots, N \quad (9)$$

Meanwhile, except for frequency restoration, we also expect our designed controller has the ability to allocate the real power sharing in an optimal ratio rather than fixed by the droop gains, i.e.,

$$\lim_{t\to\infty}\frac{P_i(t)}{P_j(t)} = \frac{\eta_i}{\eta_j} \quad (10)$$

where η_i, η_j are the optimal power sharing ratio determined by the tertiary optimization algorithm.

There are some centralized or distributed control approaches reported in literature to achieve both objectives (8) and (9). However, as pointed out before, these methods require information communication among DG secondary controllers. In the next section, a totally decentralized control scheme without communication will be proposed.

3 Decentralized secondary control for frequency restoration and optimal power sharing control

In this section, a new decentralized secondary frequency method is proposed for an islanded AC MG system. Each DG is directly controlled by the droop function based primary controller. A secondary control signal u_i is designed to add into the primary control model (4) , i.e.,

$$\tau_{pi}\dot{\omega}_i + \omega_i - \omega^d + k_{P_i}(P_i - P_i^d) + u_i = 0 \quad (11)$$

3.1 Controller design

The frequency error e^{ω_i} for the i^{th} DG is defined as follows

$$e^{\omega_i} = \omega_i - \omega^d \quad (12)$$

Motivated by the leaky integral control proposed in [14], a decentralized secondary control is designed as

$$T_i\dot{u}_i = e^{\omega_i} - K_i u_i \quad (13)$$

where $T_i \in \mathbb{R}^+$, and $K_i \in \mathbb{R}^+$ are the secondary controller parameters for the i^{th} DG.

Note that the designed decentralized controller (13) is nothing new but a leaky integral controller, which only needs the information of local frequency output ω_i. In order to simplify the stability analysis, we make the following assumption.

Assumption 1 Assume $P_i^d = 0, \forall i = 1, \cdots, N$, and there exists a synchronous solution (e^{ω^*}, P_i^*, u_i^*) for (11) and (13) in the following form:

$$e^{\omega^*} + k_{P_i}P_i^* + u_i^* = 0 \quad (14)$$

$$0 = e^{\omega^*} - K_i u_i^* \quad (15)$$

where $e^{\omega^*} = \omega_{ss} - \omega^d$ are the synchronous frequency error, P_i^* and u_i^* denote the steady-state values of real power output P_i and secondary control input u_i respectively. With Assumption 1, (6) and (7), we could get

$$(1 + K_i^{-1})e^{\omega^*} + k_{P_i}P_{L_i}^* = -k_{P_i}\hat{P}_i^* \quad (16)$$

Note that (16) is an MG network model of loss-less power transmission lines modeled in (5) with real power injections $-(1 + K_i^{-1})e^{\omega^*} - k_{P_i}P_{L_i}^*$. Referring to [14], Assumption 1 guarantees (16) to be always solvable with sufficiently small $||k_{P_i}P_{L_i}^*||$. At the steady state, (16) further implies that

$$\frac{P_i^*}{P_j^*} = \frac{k_{P_j}(1 + K_i^{-1})}{k_{P_i}(1 + K_j^{-1})} \quad (17)$$

Consider the closed-loop system (11)-(13). The synchronous frequency error e^{ω^*} can be regulated to a band around zero that can be made arbitrarily small by choosing the gains $K_i > 0$ sufficiently small.

In particular,

$$e^{\omega^*} = \left|\frac{\sum_{i=1}^{N} k_{P_i}P_i^*}{\sum_{i=1}^{N}\left(1 + K_i^{-1}\right)}\right| \quad (18)$$

Then for any $\epsilon > 0$, if

$$\sum_{i=1}^{N} K_i^{-1} \geq \frac{\sum_{i=1}^{N} k_{P_i}P_i^*}{\epsilon} - N \quad (19)$$

then

$$||e^{\omega^*}|| \leq \epsilon \quad (20)$$

In addition, from (17), we can conclude that by properly choosing K_i, the real power output can be also regulated to arbitrary ratio rather than the inverse proportion of the droop gains k_{P_i}. Specifically, if we aim to achieve the goal in (10), K_i can be chosen as

$$\frac{k_{P_j}(1 + K_i^{-1})}{k_{P_i}(1 + K_j^{-1})} = \frac{\eta_i}{\eta_j} \quad (21)$$

Clearly as a special case, it is also noted that if the secondary control only needs to maintain the power sharing ratio brought by the primary droop function, then K_i can be set as $K_i = K_j, \forall i = j = 1, \cdots, N$.

3.2 Stability Analysis

We now analyze the stability of proposed decentralized secondary controller.

Theorem 1 Consider the closed-loop system (11) - (13). Under Assumption 1, the equilibrium ($e^{\omega_i^*}$,P_i^*,u_i^*) is locally exponentially stable, if the matrix A given in (22) has exactly one zero eigenvalue and all its other eigenvalues are in the open left half complex plane.

$$A=\left[\begin{array}{ccc}\mathbf{0}_{N\times N} & \Pi & \mathbf{0}_{N\times N}\\ -\tau_P^{-1}K_P\mathcal{B}\Gamma\cos\left(\mathcal{B}^T\theta^*\right)\mathcal{B}^T & -\tau_P^{-1} & -\tau_P^{-1}\\ \mathbf{0}_{N\times N} & T^{-1} & -T^{-1}K\end{array}\right] \tag{22}$$

***Proof*:** The closed-loop system (11) - (13) can be written in the following compact form:

$$\left\{\begin{array}{c}\dot{\delta}=e^{\omega}\\ \tau_P\dot{e}^{\omega}=-e^{\omega}-K_P\mathcal{B}\Gamma\sin\left(\mathcal{B}^T\delta\right)-K_PP_L-u\\ T\dot{u}=e^{\omega}-Ku\end{array}\right. \tag{23}$$

where $e^{\omega}=col(e^{\omega_1},\cdots,e^{\omega_N})\in\mathbb{R}^{N\times 1}$, $\tau_P=diag\{\tau_{P_1},\cdots,\tau_{P_N}\}$, $K_P=diag\{k_{P_1},\cdots,k_{P_N}\}$, $P_L=col(P_{L_1},\cdots,P_{L_N})$, $\delta=col(\delta_1,\cdots,\delta_N)$, $u=col(u_1,\cdots,u_N)$, $T=diag\{T_1,\cdots,T_N\}$ $K=diag\{K_1,\cdots,K_N\}$, $\mathcal{B}\in\mathbb{R}^{N\times M}$ is the incidence matrix, $\Gamma\in\mathbb{R}^{M\times M}$ is a diagonal matrix with its diagonal entries being all the nonzero H_{ik}.

Note that the dynamics (23) is not dependent on the value of the angle δ_i but only on the difference $\delta_i-\delta_j$. For ease of later analysis, a change of coordinates for voltage phase angle δ is introduced, i.e., $\theta=\delta-\frac{1}{N}\mathbf{1}_{N\times 1}\mathbf{1}_{N\times 1}^T\delta=\Pi\delta$, where $\Pi=I-\frac{1}{N}\mathbf{1}_{N\times 1}\mathbf{1}_{N\times 1}^T$. Note that $\mathcal{B}^T\Pi=\mathcal{B}^T$, then (23) becomes

$$\left\{\begin{array}{c}\dot{\theta}=\Pi e^{\omega}\\ \tau_P\dot{e}^{\omega}=-e^{\omega}-K_P\mathcal{B}\Gamma\sin\left(\mathcal{B}^T\theta\right)-K_PP_L-u\\ T\dot{u}=e^{\omega}-Ku\end{array}\right. \tag{24}$$

Let $(\theta^*,e^{\omega^*},u^*)$ be the equilibrium of (24), which satisfies

$$\left\{\begin{array}{c}\Pi e^{\omega^*}=\mathbf{0}_{N\times 1}\\ e^{\omega^*}+K_P\mathcal{B}\Gamma\sin\left(\mathcal{B}^T\theta^*\right)+K_PP_L+u^*=\mathbf{0}_{N\times 1}\\ e^{\omega^*}-Ku^*=\mathbf{0}_{N\times 1}\end{array}\right. \tag{25}$$

From the first equation in (25), it can be concluded that $e^{\omega^*}=c\mathbf{1}_{N\times 1}$, where c is an arbitrary number. This indicates that the frequency error will synchronize to a constant value. As also seen from the second and third equations in (25), e^{ω^*} can be set arbitrarily small by choosing sufficiently small gain K. In addition, the equations are consistent with (16) and (15) respectively.

We now show that (24) is locally exponentially stable. By linearizing (24) around the equilibrium $(\theta^*,e^{\omega^*},u^*)$, we obtain

$$\left[\begin{array}{c}\Delta\dot{\theta}\\ \Delta\dot{e}^{\omega}\\ \Delta\dot{u}\end{array}\right]=A\left[\begin{array}{c}\Delta\theta\\ \Delta e^{\omega}\\ \Delta u\end{array}\right] \tag{26}$$

where $\Delta\theta=\theta-\theta^*$, $\Delta e^{\omega}=e^{\omega}-e^{\omega^*}$, $\Delta u=u-u^*$ and A is given in (22).

By calculation, we obtain that $A\mathbf{e}_1=\mathbf{0}_{N\times N}$, where $\mathbf{e}_1=\left[\begin{array}{ccc}\mathbf{1}_{1\times N} & \mathbf{0}_{1\times N} & \mathbf{0}_{1\times N}\end{array}\right]^T$ is an eigenvector of A corresponding to the eigenvalue 0, which indicates that A has at least one eigenvalue equals 0. Next we will show that it has exactly one zero eigenvalue.

Consider the following linear coordinate transform

$$\Delta\theta'=\mathcal{R}\Delta\theta,\ \ \Delta e^{\omega'}=\mathcal{R}\Delta e^{\omega},\ \ \Delta u'=\mathcal{R}\Delta u \tag{27}$$

where

$$\mathcal{R}=\left[\begin{array}{c}\frac{1}{\sqrt{N}}\mathbf{1}_{1\times N}\\ \mathcal{S}^T\end{array}\right] \tag{28}$$

with $\mathcal{S}$ being a matrix such that $\mathcal{R}$ is an orthonormal matrix. Then in the new coordinate, system (26) can be described as

$$\Delta\dot{\theta}'=\left[\begin{array}{cc}0 & \mathbf{0}_{1\times(N-1)}\\ \mathbf{0}_{(N-1)\times 1} & \mathcal{S}^T\Pi\mathcal{S}\end{array}\right]\Delta e^{\omega'} \tag{29}$$

$$\begin{aligned}\Delta\dot{e}^{\omega'}=&-\mathcal{R}\tau_P^{-1}K_P\mathcal{B}\Gamma\cos(\mathcal{B}^T\theta^*)\left[\begin{array}{cc}\mathbf{0}_{M\times 1} & \mathcal{B}^T\mathcal{S}\end{array}\right]\Delta\theta'\\ &-\mathcal{R}\tau_P^{-1}\mathcal{R}^T\Delta e^{\omega'}-\mathcal{R}\tau_P^{-1}\mathcal{R}^T\Delta u'\end{aligned} \tag{30}$$

$$\Delta\dot{u}'=\mathcal{R}T^{-1}\mathcal{R}^T\Delta e^{\omega'}-\mathcal{R}T^{-1}K\mathcal{R}^T\Delta u' \tag{31}$$

It is observed from (29) and (30) that the state $\Delta\theta_1'$ is both uncontrollable and unobservable. In order to obtain a minimal realization, we omit state $\Delta\theta_1'$ by defining the new coordinate as $\Delta\theta''=[\Delta\theta_2',\cdots,\Delta\theta_N']^T\in\mathbb{R}^{(N-1)\times 1}$. Then system (29) -(31) can be re-written as

$$\left[\begin{array}{c}\Delta\dot{\theta}''\\ \Delta\dot{e}^{\omega'}\\ \Delta\dot{u}'\end{array}\right]=A'\left[\begin{array}{c}\Delta\theta''\\ \Delta e^{\omega'}\\ \Delta u'\end{array}\right] \tag{32}$$

where A' is given in (33).

Now we will show that A' is a full-rank matrix. Considering

$$A'\left[\begin{array}{c}\mathbf{x}_1\\ \mathbf{x}_2\\ \mathbf{x}_3\end{array}\right]=\mathbf{0}_{(3N-1)\times 1} \tag{34}$$

where $\mathbf{x}_1\in\mathbb{R}^{(N-1)\times 1}$, $\mathbf{x}_2\in\mathbb{R}^{N\times 1}$, $\mathbf{x}_3\in\mathbb{R}^{N\times 1}$, we have the relationships shown in (35).

From (35), it is easy to conclude that $\left[\begin{array}{c}\mathbf{x}_1\\ \mathbf{x}_2\\ \mathbf{x}_3\end{array}\right]=\mathbf{0}_{(3N-1)\times 1}$ is the only solution of (34), thus, A' is of full rank. Hence, A' is Huwritz if and only if A has exactly one zero eigenvalue and all others are in the open left half complex plane. Thus the overall system (11)-(13) is locally exponentially stable. This completes the proof.

4 Simulation Results

In this section, in order to validate the effectiveness of the designed secondary controller, a test islanded MG system consisting of 4 DGs is built up in Matlab Simulink. The power system connection is set the same as that in [15].

$$A' = \begin{bmatrix} \mathbf{0}_{(N-1)\times(N-1)} & \begin{bmatrix} \mathbf{0}_{(N-1)\times 1} & \mathcal{S}^T\Pi\mathcal{S} \end{bmatrix} & \mathbf{0}_{(N-1)\times N} \\ -\mathcal{R}\tau_P^{-1}K_P\mathcal{B}\Gamma\cos\left(\mathcal{B}^T\theta^*\right)\mathcal{B}^T\mathcal{S} & -\mathcal{R}\tau_P^{-1}\mathcal{R}^T & -\mathcal{R}\tau_P^{-1}\mathcal{R}^T \\ \mathbf{0}_{N\times(N-1)} & \mathcal{R}T^{-1}\mathcal{R}^T & -\mathcal{R}T^{-1}K\mathcal{R}^T \end{bmatrix} \tag{33}$$

$$\begin{cases} \begin{bmatrix} \mathbf{0}_{(N-1)\times 1} & \mathcal{S}^T\Pi\mathcal{S} \end{bmatrix}\mathbf{x}_2 = \mathbf{0}_{(N-1)\times 1} \\ -\mathcal{R}\tau_P^{-1}K_P\mathcal{B}\Gamma\cos\left(\mathcal{B}^T\theta^*\right)\mathcal{B}^T\mathcal{S}\mathbf{x}_1 - \mathcal{R}\tau_P^{-1}\mathcal{R}^T\mathbf{x}_2 - \mathcal{R}\tau_P^{-1}\mathcal{R}^T\mathbf{x}_3 = \mathbf{0}_{N\times 1} \\ \mathcal{R}T^{-1}\mathcal{R}^T\mathbf{x}_2 - \mathcal{R}T^{-1}K\mathcal{R}^T\mathbf{x}_3 = \mathbf{0}_{N\times 1} \end{cases} \tag{35}$$

Table 1: Parameters of DG and its controllers

		DG1	DG2	DG3	DG4
DG	ω^d	50Hz	50Hz	50Hz	50Hz
Primary Controller	τ_i	0.016	0.016	0.016	0.016
	k_{pi}	6e-5	3e-5	2e-5	1e-5
Secondary Controller	K_{1i}	0.01	0.01	0.01	0.01
	T_{1i}	1e-4	1e-4	1e-4	1e-4
	K_{2i}	0.01	0.04	0.09	0.36
	T_{2i}	1e-4	1e-4	1e-4	1e-4
Load	P_{Li}	20kW	20kW	20kW	20kW

The detailed parameter configurations of these 4 DGs are summarized in Table I. In our simulation studies, the ability of decentralized frequency restoration and the power sharing control is tested. The designed controller parameters are also shown given in Table I, from which it can be calculated that the initial real power sharing ratio is $P_1 : P_2 : P_3 : P_4 = 1 : 2 : 3 : 6$.

The whole simulation could be divided into 4 stages:

Stage 1 (0-5s): only primary frequency controller is on operation;

Stage 2 (5s): the designed secondary controller is activated;

Stage 3 (10s-500s): a new local real power load power $P_{L_1} = 20kW$ is added in DG1 bus.

Stage 4 (500s-): P_{L_1} is removed from DG1 bus.

Stage 5 (1000s-): the power sharing ratio among these 4 DGs is changed to 6:3:2:1.

Initially, only primary control is on operation with initial loads $P_{L_1} = 20kW$, $P_{L_2} = 20kW$, $P_{L_3} = 20kW$, $P_{L_4} = 20kW$. The simulation results are shown in Figs. 1 and 2. As observed from Fig. 1(b), during the first 3 seconds, the frequency is synchronized to about 49.6 Hz, which is deviated from the nominal 50 Hz. The power output is shown in Fig. 2 (b), where inverse proportion of droop gains is achieved. After the secondary controller is activated, the frequency is quickly restored to around 50Hz and the power sharing ratio is kept the same. In addition, at $t = 10s$, an extra local real power load $P_{L_1} = 20kW$ is added in DG1 bus. It can be seen from Fig. 1 (c) that the frequency of DG1 has a transient oscillation but can finally recover to around 50 Hz. When P_{L_1} is removed from DG1 local bus at $t = 500s$, similarly as observed from Fig. 1 (d), after around $50s$ the system frequency can still synchronize to around 50 Hz. It is also observed from Fig. 2 (a) that no matter P_{L_1} is added or removed, the power sharing ratio is kept the same as that in Stage 1 (only with primary control). At Stage 5, assume that due to the working condition changing, the power sharing ratio among these 4 DGs is changed to $6 : 3 : 2 : 1$. In this case, according to (21), by changing the value of K_i (here K_i is chosen as K_{2i} listed in Table I), such power sharing control can be achieved.

It is also worthy to point out that there exists a trade-off between the transient performance and the steady-state error. Generally, larger K_i and T_i would result in a quicker transient response but larger steady-state frequency error. In addition, as observed from our simulation results, compared to the distributed control approach in [15], the proposed decentralized control method results in a bounded steady-state error and has slower transient response. But no information communication is required in this decentralized approach, which would be more beneficial in terms of cost saving and security, robustness and economic.

5 Conclusion

In this paper, a decentralized leaky integral control approach for AC MG frequency restoration is presented. It is theoretically proved that the proposed controller not only restores the system frequency, but also changes the power sharing ratio by setting different control parameters online. Simulation test results validate our theoretical findings.

REFERENCES

[1] F. A. Ipakehi, "Grid of the future," *IEEE Power Energy Mag.*, vol. 7, no. 2, pp. 5262, Mar. 2009.

[2] F. Guo, Q. Xu, C. Wen, L. Wang and P. Wang,"Distributed Secondary Control for Power Allocation and Voltage Restoration in Islanded DC Micgrid," *IEEE Transactions on Sustainable Energy*, vol. 9, no.4, pp. 1857-1869, March. 2018.

[3] J. Schiffer, D. Zonetti, "A survey on modeling of microgrids From fundamental physics to phasors and voltage sources," *Automatica*, vol.74, pp. 135-150, Dec. 2016.

[4] J. M. Guerrero, J. C. Vasquez, R. Teodorescu, "Hierarchical control of droop-controlled ac and dc microgridsA general approach toward standardization, *Industrial Electronics, Conference of IEEE*, pp. 4305-4310, 2009.

[5] M. Saleh, Y. Esa, A. A. Mohamed, "Communication-based control for DC microgrids," *IEEE Transactions on Smart Grid* , vol.10, no. 2, pp. 2180-2195, 2019.

[6] M. Yazdanian and A.Mehrizi-Sani, "Distributed control techniques in microgrids," *IEEE Transactions on Smart Grid*, vol. 5, no. 6, pp. 2901-2909, Aug. 2014.

[7] Q. Shafiee, J. M, Guerrero, and J. L. Vasquez , "Distributed secondary control for islanded microgrid- A novel approach,"

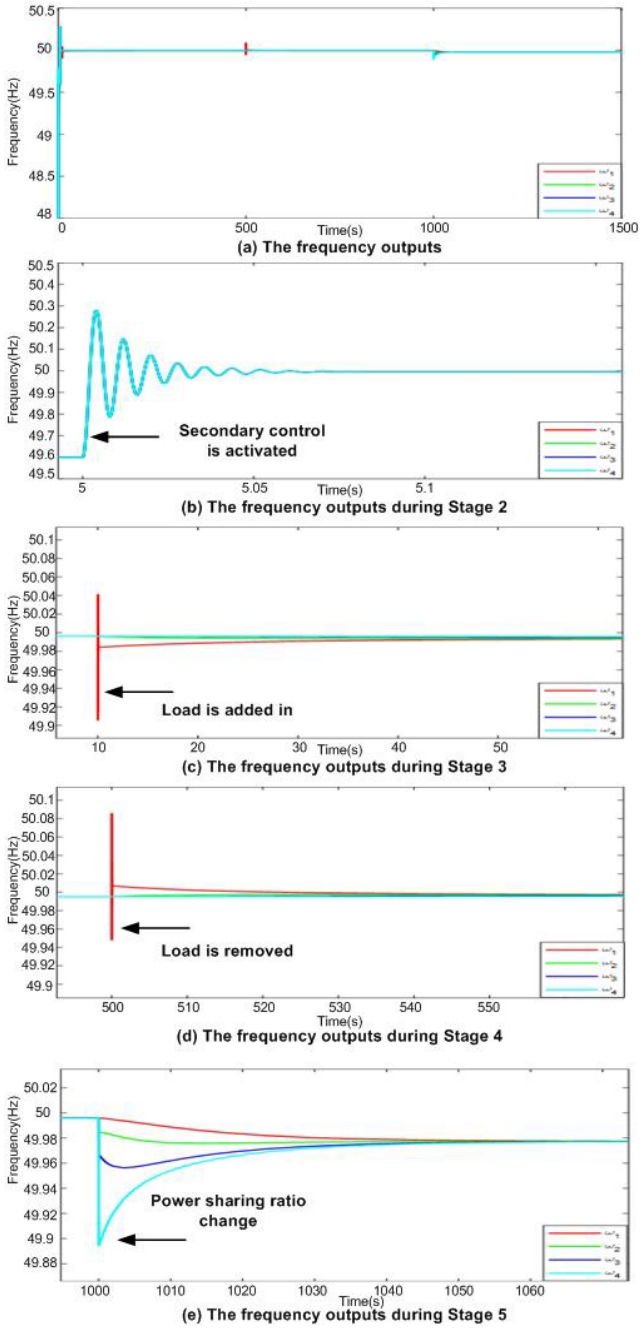

Figure 1: The frequency outputs of 4 DGs

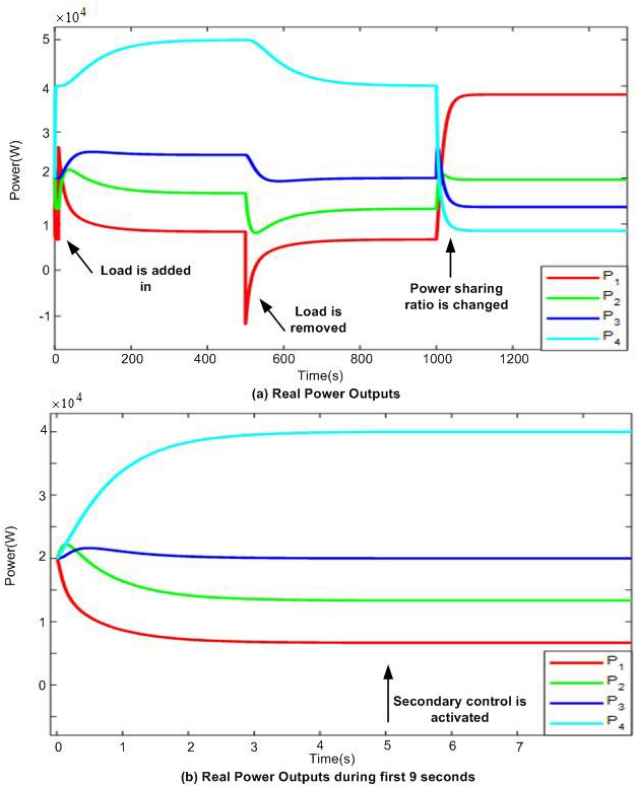

Figure 2: The real power outputs of 4 DGs

IEEE Transactions on Power Electronics, vol. 29, no. 2, pp.1018 - 1031, Feb. 2014.

[8] F. Guo, C. Wen, J. Mao, J. Chen and Y.-D. Song, "Distributed cooperative secondary control for voltage unbalance compensation in an islanded microgrid," *IEEE Transactions on Industrial Informatics*, vol. 11, no. 5, pp. 1078 - 1088, Oct., 2015.

[9] W. Liu, P. Zhuang, H. Liang , J. Peng and Z. Huang, "Distributed economic dispatch in microgrids based on cooperative reinforcement learning," *IEEE Transactions on Neural Networks and Learning Systems*, vol. 29, no. 6, pp. 2192 - 2203, June 2018.

[10] J. M. Guerrero, M. Chandorkar, T. Lee, and P. C. Loh, "Advanced control architectures for intelligent microgrids -Part I: Decentralized and hierarchical control, *IEEE Transactions on Industrial Electronics*, vol. 60, no. 4, pp. 12541262, Apr. 2013.

[11] L. Dong, Y. Zhang, Z. Gao, "A robust decentralized load frequency controller for interconnected power systems," *ISA Transactions*, vol. 51, no. 3, pp. 410-419 , May. 2012.

[12] M. Savaghebi, A. Jalilian, J. C. Vasquez and J. M. Guerrero, "Decentralized optimal frequency control in autonomous microgrids," *IEEE Transactions on Power Systems*, published online, DOI: 10.1109/TPWRS.2018.2889671, Dec. 2018.

[13] J. A. P. Lopes, C. L. Moreira, and A. G. Madureira, "Agent-based decentralized control method for islanded microgrids," *IEEE Transactions on Smart Grid*, vol. 7, no. 2, pp. 637-649, Mar. 2016.

[14] E. Weitenberg, Y. Jiang, C. Zhao, E. Mallada, C. De Persis, "Robust decentralized secondary frequency control in power systems: Merits and trade-offs," *IEEE Transactions on Automatic Control*, published online, DOI: 10.1109/TAC.2018.2884650, Dec., 2018.

[15] F. Guo, C. Wen, J. Mao and Y.-D. Song, "Distributed secondary voltage and frequency restoration control of droop-controlled inverter-based microgrids," *IEEE Transactions on Industrial Electronics*, vol. 62, no. 7, pp. 4355 - 4364, July, 2015